DOI: 10.1002/chem.200501520

Calixarenes as Hosts for Ammonium Cations: A Quantum Chemical Study and Mass-Spectrometric Investigations

Alexander B. Rozhenko, Wolfgang W. Schoeller,* Matthias C. Letzel, Björn Decker, Ceno Agena, and Jochen Mattay[a]

Abstract: Host–guest complexes of tetramethylcavitand with different ammonium cations were investigated by using a quantum chemical method at the density functional level (BP86, B3LYP). The NH_4^+ cation is strongly bound to the host. Increasing methyl substitution at the cation decreases its inclination towards the complex formation. The calculated data are in line with results from electrospray ionization mass spectrometry (ESI-MS) experiments. They reveal stable aggregates only for the NH_4^+ cation and for the primary alkylammonium cations.

Keywords: ammonium cations · cavitands · density functional calculations · host–guest systems · mass spectrometry

Introduction

The design of selectively and effectively bound host–guest aggregates is the challenge of supramolecular chemistry. Calix[4]arenes and structurally similar cavitands are potent and size-selective receptors for a variety of substrates, in particular, for inorganic and organic cations.[1,2] A variety of inclusion complexes of calix[4]arenes with metal cations were investigated experimentally[3] as well as theoretically.[4] The corresponding aggregates are bound predominantly by electrostatic interactions. The inclusion of alkylammonium cations as cationic guests mimics some bioorganic processes, such as the recognition of the acetylcholine by acetylcholinesterase, based on cation–π interactions.[5,6] The first detailed experimental study of complexes was reported for the system of tetraphenolate of resorc[4]arenes with a series of quaternary ammonium cations.[7] The structures for some inclusion complexes were also investigated in the solid state.[8,9] The cations formed complexes with the ligands, which also involved solvent molecules.[8] In the structure of the complex of the anionic sulfonatocalix[4]arene with the tetramethylammonium ion published by Atwood et al.,[9] the negative charge of the sulfonic groups attracted the positively charged cation. In contrast, the neutral calix[4]arene did not react with quaternary ammonium salts in solution.[10] Irico et al.[11] found significant interactions with a series of ammonium cations only for the phosphate-bridged cavitands that carried at least three P=O groups oriented inside the cavity.

In contrast to the cavitands, their relatives, calix[4]arenes, build stable aggregates with the (alkyl)ammonium cations. In most cases, the ligands were modified with the SO_3^- groups to provide stronger interaction with the positively charged guest. The ammonium cation NH_4^+ did not form stable aggregates with *p*-sulfonatocalix[4]arene.[12] In the NH_4^+ ion, the positive charge is localized predominantly at the hydrogen atoms that are optimal for an effective cation–π interaction, but it is strongly mediated by protic solvents. The larger, but less-solvated Me_4N^+ cation dived deeply into the cavity to form a stable aggregate. In case of the Et_4N^+ cation or Pr_4N^+ cation, the only alkyl chain was directed inside the cavity. Interestingly, for the cations R_4N^+ with longer alkyl groups (R = Et, *n*Pr, *n*Bu), the nitrogen atom remained outside the cavity. Only cations with a single alkyl group evidenced ammonium inclusion. Perret et al.[13] investigated a series of alkylammonium salts RNH_3^+ (R: Me to Hept) and found that the enthalpy of binding became more favourable as the length of the alkyl chain increased. The most negative enthalpy (ca. $-20\,kJ\,mol^{-1}$) was for $PentNH_3^+$ and was interpreted as evidence that the pentyl group fitted best into the cavity. In this case, a conformation was assumed in which the alkyl moiety dived inside of the calixarene cavity. If the aromatic moiety was present in the cation structure, the competitive π–π interaction made the

---

[a] Dr. A. B. Rozhenko, Prof. Dr. W. W. Schoeller, Dr. M. C. Letzel,
B. Decker, C. Agena, Prof. Dr. J. Mattay
Fakultät für Chemie, Universität Bielefeld
33615 Bielefeld (Germany)
Fax: (+49) 521-106-6467
E-mail: wolfgang.schoeller@uni-bielefeld.de

Supporting information for this article is available on the WWW under http://www.chemeurj.org/ or from the author.

aryl inclusion preferable to the cation–π interaction model.[14a] In these cases, the host accepted the *flattened cone* conformation.

All attempts to find stable complexes of the neutral cavitands with (alkyl)ammonium cations have so far failed, however, this is not evidence of their overall instability. Until now, the detailed aspects of the host–guest interactions in this case are not clear. To the best of our knowledge, complexation of cavitands with ammonium cations was not investigated by using quantum chemical methods. Several semiempirical calculations and molecular dynamics simulations were reported for a selected variety of ammonium cations[12,14] with calix[4]arenes, with and without anionic groups at the upper rim of cyclophane hosts. Although these studies have their own merit, they suffer from the inaccuracy of the semiempirical force field used for the structure calculation.

The diversity of experimental data raised our interest in a further rationale of the complexation process. Here, we report on the geometries for aggregates **2**–**9** (Scheme 1), to reveal the factors that contribute to the stabilities of the complexes of cavitand **1**. We show that not only the volume of the cavitand cavity and ammonium cation, but also the character of substitution at the nitrogen moiety play decisive roles in complex formation. The O−CH$_2$−O bridges in **1** fixed the structure and prevented a large diversity of conformations. Our study is based on the density functional theory (DFT).[15] Although van der Waals interactions are poorly described by DFT methods, the latter provide reliable structures and reaction enthalpies for the formation of adducts based on the cation–π interactions. This was proven by previous investigations that focused on the inclusion of calixarenes[16] and even their dimers.[17] In all cases, the mass-spectrometric investigation results were in good agreement with the calculation data.

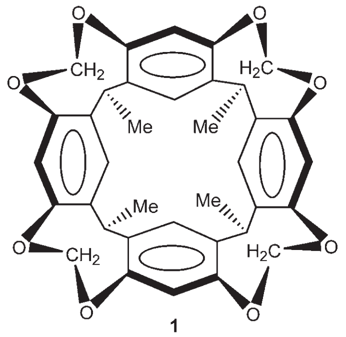

1

2: [**1** · NH_4]$^+$
3: [**1** · $MeNH_3$]$^+$
4: [**1** · $EtNH_3$]$^+$
5: [**1** · *n*$PrNH_3$]$^+$
6: [**1** · Me_2NH_2]$^+$
7: [**1** · Me_3NH]$^+$
8: [**1** · Me_4N]$^+$
9: [**1** · $EtNMe_3$]$^+$

Scheme 1.

Computational Details

All of the structures were fully optimized without symmetry constraints, with the exception of **1**, which was constrained to C_4 symmetry. We used the BP86 functional[18,19] with the Resolution of the Identity (RI)[20] algorithm implemented in the TURBOMOLE program package.[21] The implemented split-valence basis set SV(P)[22] was used, (7s4p)/[3s2p] for C, N, and O with the contraction {511/31} and (4s)/[2s] for H with the contraction {31}. One set of polarization functions was added for C, N, and O. A fine self-consistent field (SCF) convergence criterion (SCFConv = 1.0×10^{-8} Hartree) was used for geometry optimization. For all structures, vibration analyses were performed, computing analytical first- and second-order derivatives.[23] Some structures were recalculated with the GAUSSIAN-03[24] program sets by using the standard 6–31G* basis set[25] and the B3LYP hybrid functional,[26,27] to ascertain whether the two DFT methods provide comparable structures by geometry optimization. In all cases, the finest grids were used for all calculations (grid = 5 for TURBOMOLE and Grid = Ultrafine for GAUSSIAN). No vibration analyses were performed for the structures calculated with the B3LYP functional. A full account for the optimized geometries is given in the Supporting Information. The structures were also optimized with the force fields (Dreiding[28] and UFF[29]) and semiempirical (PM3[30]) methods implemented in the GAUSSIAN-03 package of programs. Although the equilibrium structures are close to those calculated at the DFT level of theory, the relative stabilities predicted by all methods mentioned did not agree with the experimental data (Supporting Information, Table S2). Therefore, the corresponding data are not considered further in the Discussion. Single-point energy calculations were performed by using the TURBOMOLE program at the DFT (RI-BP86) level of approximation. The geometries optimized at the DFT [RI-BP86/SV(P)] level of approximation and the high-quality basis sets[31] [(11s6p)/[5s3p] for C, N, and O with the contraction {62111/411} and (5s)/[3s] for H contracted as {311}] were used for the energy calculation. Three sets of polarization functions were added for C, N, and O (2d,1f) and for H (2p,1d) (TZVPP basis sets implemented in the TURBOMOLE packet). The basis set superposition error (BSSE) values were calculated for the TZVPP basis set for different ammonium complexes. The RI-BP86/TZVPP single-point energy calculation was performed for the cavitand structure cut from the ammonium complexes in either the presence or absence of the ammonium cation basis functions. The same procedure was repeated for the ammonium parts of the molecules. The latter contributions were rather small and did not play any significant role in our calculations. The energy differences were summed to calculate the BSSE values. These did not exceed 0.7 kcal mol^{-1} at the chosen level of approximation. Reaction energies were corrected by the zero-point energies at the RI-BP86/SV(P) level without scaling. The VMD program packet[32] was used for the graphical presentation of the calculated structures.

Results and Discussion

Plots of the calculated structures are shown in Figure 1. The equilibrium cavitand **1** structure adopted C_4 symmetry. To achieve an effective cation–π interaction, one should take into account the following aspects: a) a positive charge should be localized at the atoms or groups that dive into the cavity; b) distance(s) between the positively charged center and the π system(s) (cation–C^{arom}) should be maintained at optimum. Here, we will consider the distances to the carbon atom at the upper (C^{up}), the ones next to this (C^{next}), and that at the lower rim of the cavity (C^{low}) (Scheme 2).

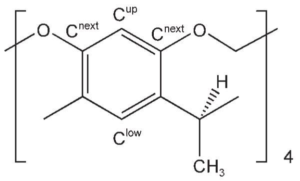

Scheme 2. Carbon atom denotation in the aromatic rings of calix[4]arene.

Complexation of RNH_3^+ (R=H, Me, Et): A positive charge in NH_4^+ is localized predominantly at the hydrogen atoms. The structures **2a** and **2b** (Figure 1) correspond to the two different complexation modes. These depend on the number of the hydrogen atoms interacting with the π systems. Both conformations are characterized by almost the same total energies, calculated with either the BP86 or B3LYP functionals. In the first conformation, three hydrogen atoms are inside the cavity, whereas the fourth hydrogen does not participate in binding. In the case of **2b**, all four hydrogen atoms are bound. In both cases, the nitrogen dives deeply into the calixarene cavity. The distance between the nitrogen and the carbon atom C^{up} at the upper rim (4.0–4.1 Å) is even larger than that to C^{low} (3.2 Å). The situation does not change significantly following substitution of one hydrogen in **2a** with a methyl group (Figure 1, **3a**): the nitrogen atom remains deep inside the cavity (this situation will be further designated as the "ammonium inside" mode of complexation) and the methyl group in **3a** (or the α-CH_2 group in the cases of **4a** and **5a**) (Figure 1) is positioned at the upper rim of the calixarene. The residue of the alkyl substituent (in cases of **4a** and **5a**) is outside the cavity.

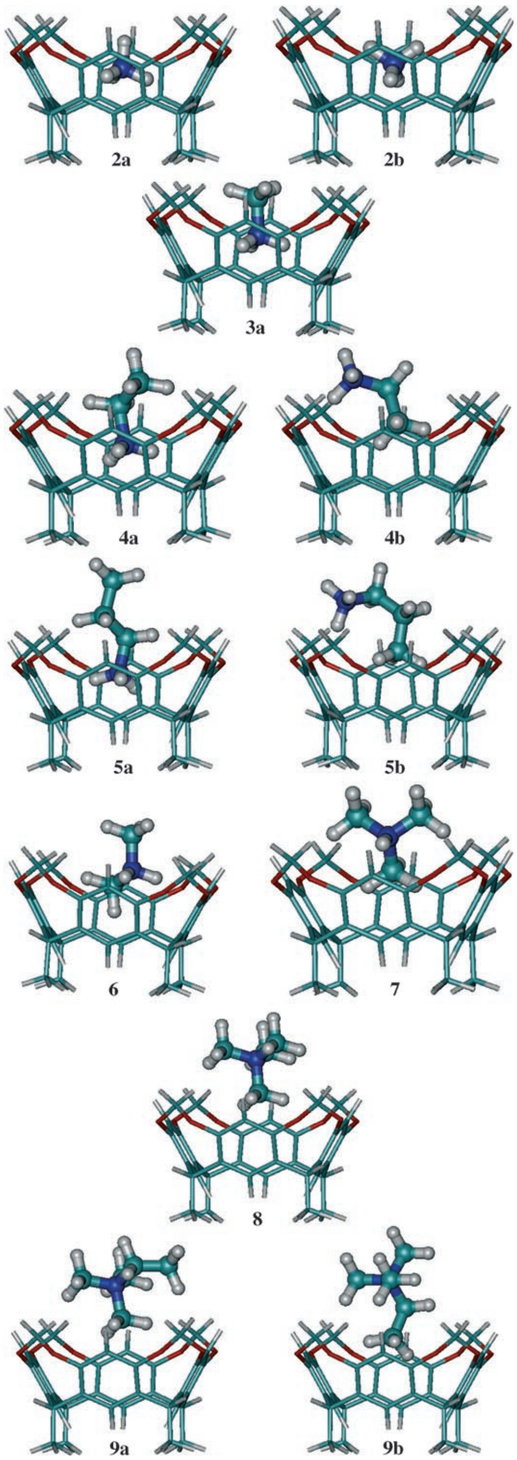

Figure 1. Graphical representation of cavitand **1** in complexes with NH_4^+ (**2a** and **2b**), $MeNH_3^+$ (**3a**), $EtNH_3^+$ (**4a** and **4b**), *n*$PrNH_3^+$ (**5a** and **5b**), $Me_2NH_2^+$ (**6**), Me_3NH^+ (**7**), Me_4N^+ (**8**), and $EtNMe_3^+$ (**9a** and **9b**).

We also optimized the geometries for the alternative conformations with the alkyl group inside the cavity and the ammonium remainder, pointing outside the calixarene cup (further designated as "alkyl inside" mode of complexation). The adduct with $MeNH_3^+$ as a guest remained unstable in this conformation by energy optimization and relaxed back to **3a**. The reason becomes clear after analysis of the next members of this series, **4b** and **5b**, located as minima in energy. Only the Me group remains inside the cavity. The rest of the alkyl chain is oriented in such a way that the NH_3 group approaches three upper carbon atoms of the aromatic ring. The particular short NH–C^{up} distances of 2.05 (**4b**) and 2.09 Å (**5b**) and NH–C^{next} distances (2.55 to 2.67 Å) indicate practically a η^3 coordination for the hydrogen.[33] Such a conformation is not stable for the adduct with $MeNH_3^+$. The total-energy values that we computed (Reac-

Table 1. Calculated (RI-BP86/TZVPP//RI-BP86/SV(P)) total-energy values and Reaction (1) energies ($T=298$ K) for **1**–**9**.

Compound	Guest	Total energy, E [a.u.]	ZPE correction [a.u.][a]	$E+ZPE$ [a.u.]	ΔE [kcal mol^{-1}]	Thermal correction (TC) to ΔG [a.u.][a]	E+TC [a.u.]	ΔG [kcal mol^{-1}]	Lowest vibration, ν [cm^{-1}]
1	–	–1993.690417	0.597459	–1993.092958	0.0	0.474679	–1993.215738	–	30.3
1a	–	–1992.839392	–	–	0.0	–	–	–	–
2a	NH_4^+	–2050.666918	0.645203	–2050.021715	–30.2				31.6
2a[b]	NH_4^+	–2049.779845	–	–	–29.2	–			–
2b	NH_4^+	–2050.666834	0.645855	–2050.020980	–29.7	0.513940	–2050.152894	–20.1	33.1
2b[b]	NH_4^+	–2049.781020	–	–	–30.0	–	–	–	–
3a	$MeNH_3^+$	–2089.988783	0.674138	–2089.314645	–28.0	0.536743	–2089.452039	–17.6	36.5
4a	$EtNH_3^+$	–2129.318866	0.702062	–2128.616804	–20.3	0.560891	–2128.757975	9.0	42.2
4a[b]	$EtNH_3^+$	–2128.412854	–	–	–22.6	–	–	–	–
4b	$EtNH_3^+$	–2129.296627	0.701354	–2128.595273	–6.8	0.560529	–2128.736097	4.7	30.7
4b[a]	$EtNH_3^+$	–2128.390028	–	–	–8.3	–	–	–	–
5a	$PrNH_3^+$	–2168.647225	0.729681	–2167.917545	–19.5	0.582971	–2168.064255	–8.3	17.6
5a[b]	$PrNH_3^+$	–2167.727740	–	–	–22.1	–	–	–	–
5b	$PrNH_3^+$	–2168.621276	0.728876	–2167.892400	–3.7	0.582586	–2168.038689	7.7	31.5
5b[b]	$PrNH_3^+$	–2167.701073	–	–	–5.3	–	–	–	–
6	$Me_2NH_2^+$	–2129.301147	0.701926	–2128.599221	–13.8	0.560739	–2128.740408	–2.5	39.9
7	Me_3NH^+	–2168.614809	0.729750	–2167.885059	–4.5	0.584692	–2168.030116	–4.5	39.3
8	Me_4N^+	–2207.931323	0.755609	–2207.175714	0.4	0.605233	–2207.326090	11.6	–4.9
9a	$EtNMe_3^+$	–2247.260620	0.783387	–2246.477233	1.5	0.626471	–2246.634149	11.8	25.7
9b	$EtNMe_3^+$	–2247.260258	0.783371	–2246.476887	1.7	0.626285	–2246.633973	11.9	13.9

[a] Calculated at the RI-BP86/SV(P) level of approximation, without scaling. [b] Structures were optimized at the B3LYP/6–31 g* level. No vibrational analyses were performed in these cases and also no zero-point corrections were applied for the calculations of ΔE.

tion (1)) refer to the gas phase and can not be taken as a quantitative measure for coordination in solution.

$$\mathbf{1} + \text{ammonium}^{(+)} \rightarrow [\text{complex}]^{(+)} + \Delta E \qquad (1)$$

In the usual experiment, the cation and the free cavitand are solvated effectively by polar protic solvents. The calculated ΔG values obtained from a statistical thermodynamic treatment (Table 1) also refer to the gas phase and change in accordance with the ΔE magnitudes. However, an exothermic effect obtained for Reaction (1) is approximately 10 kcal mol^{-1} lower. These values neglect desolvation of the ammonium cations by formation of the adducts (with the cavitand). Thus, the ΔG values for Reaction (1) are systematically underestimated. They reveal no further advantage over the analysis based on corresponding total energies and will not be discussed here in more detail.

Complexation of $Me_2NH_2^+$, Me_3NH^+, and Me_4N^+: We have already considered the first two members of this series, complexes with NH_4^+ (**2a**,**b**) and $MeNH_3^+$ (**3a**). Because of the tetrahedral symmetry of NH_4^+ and the orientation of the single Me group to the outside of the cavitand cavity, they are characterized by an almost central position of the nitrogen atom within the ligand cup. An introduction of the additional methyl substituents significantly changes the coordination mode. The equilibrium structures of **6** and **7** are shown in Figure 1. In **6**, the nitrogen is diagonally shifted from the center of the cavity. By geometry optimization we obtained a C_s symmetrical equilibrium structure with the symmetry plane passing through the cavitand's diagonal. The nitrogen atom lies practically over the center of the aromatic rings (almost equal N–C^{up} and N–C^{down} distances (3.40 and 3.82 Å, respectively). Two available NH protons interact with the neighboring aromatic rings [d(NH–C^{up}) = 2.35 and d(NH–C^{next}) = 2.40 and 2.72 Å]. The ΔE energy changes only slightly from **2** to **3**, but Reaction (1) becomes significantly less exothermic for $[\mathbf{1}\cdot NH_2Me_2]^+$ (**6**) and especially for $[\mathbf{1}\cdot NHMe_3]^+$ (**7**). The latter complex reveals the unfavorable "alkyl inside"-type coordination discussed above. The equilibrium structure **7** is also of C_s symmetry (the symmetry plane passes through NH, two C^{up} and two C^{down} carbon atoms). The nitrogen atom is positioned closer to one of the aromatic rings (d(N–C^{up}) = 3.63 and d(N–C^{next}) = 4.49 Å) than to the other three rings and tends to be closer to the upper rim of the cavitand. The NH hydrogen is $\eta^1(\eta^3)$-connected to the upper aromatic carbon (d(NH–C^{up}) = 2.60 and d(NH–C^{next}) = 2.98 Å). These increased distances indicate that the cation–π interaction is weaker here than in all other complexes discussed previously. For **7**, the calculations also predict a lower negative reaction energy ΔE (–4.5 kcal mol^{-1}).

Does the large tetramethylammonium cation effectively interact with the π system of cavitand **1**? A priori, the positive charge is now delocalized over the 16 atoms of four Me groups and the CH–π interactions are weaker than the NH–π interaction considered above. The equilibrium structure (Figure 1, **8**) is nearly C_s symmetrical. Only one Me group is close to the upper rim of the cavitand, whereas the residual part of the molecule (including the nitrogen atom) remains outside the cavity. This is in line with the very low exothermic effect (less than 1 kcal mol^{-1}) of Reaction (1) in forming **8** (if calculated with the larger basis set TZVPP, this effect became even slightly endothermic, see Table 1). Therefore, the tetramethylammonium cation can form only very weak, if any, complexes with **1**.

Long chain versus short chain of alkyl substitution at the ammonium cation: This aspect has been partially considered above, and we have shown that longer alkyl substituents at nitrogen do not improve complexation relative to the positively charged NH_3^+ rest. Here, we consider only the complexes $[\mathbf{1}{\cdot}EtNMe_3]^+$ as an attempt to model a long alkyl-chain ammonium species. The corresponding "methyl inside" (**9a**) or "ethyl inside" (**9b**) adducts are compared with those having $EtNH_3^+$ as the guest (**4a** and **4b**, respectively). We hoped that, in line with previous experimental findings,[13] the longer alkyl chain would make "alkyl inside" complexation mode preferable. However, the "ethyl inside" inclusion complex, **9b**, turned out to possess almost the same total energy as the isomer **9a** and, hence, low exothermic reaction energies ΔE were found for both isomers. It is probable that tetraalkylammonium cations fit poorly as guests into cavitand **1**.

Electrospray ionization mass spectrometry of 2–8: The complexation of **1** with the ammonium cations was investigated by conducting electrospray mass spectrometry. First, the cavitand was mixed with an equimolar (relative to every cation) mixture of ammonium, methylammonium, dimethylammonium, trimethylammonium, and tetramethylammonium chlorides. The spectrum obtained is presented in Figure 2. Only signals corresponding to the complexes with $NH_4^{(+)}$ and $MeNH_3^{(+)}$ are apparent, with a greater abundance of the former than the latter. No complexes with $Me_2NH_2^{(+)}$, $Me_3NH^{(+)}$, and $Me_4N^{(+)}$ were detected experimentally, which is in good agreement with their lower stability predicted by our calculations.

On the other hand, in the spectrum of the mixture of tetramethylcavitand with an equimolar mixture of ammonium, methylammonium, ethylammonium, and *n*-propylammonium chlorides (Figure 3), all corresponding signals are visible. This means that, in line with our theoretical findings, the monosubstituted RNH_3^+ are able to build stable complexes with the tetramethylcavitand. The length of the alkyl chain has no significant effect on the ability of the alkylammonium cations to build complexes, although their signal intensities are significantly lower than those corresponding to the complex with NH_4^+.

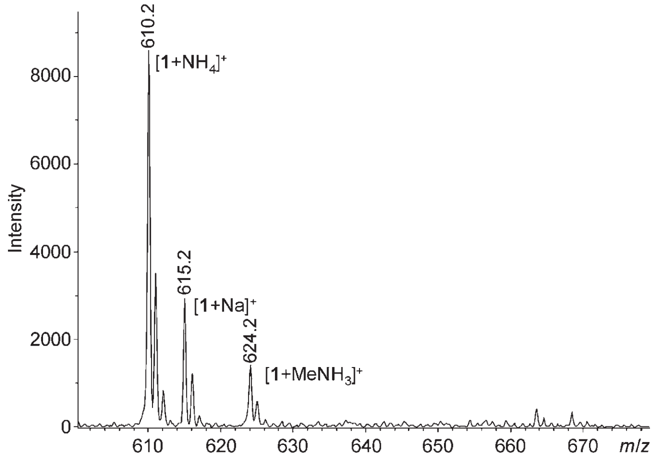

Figure 2. Electrospray mass spectrum of the tetramethylcavitand (X) in a mixture with an equimolar amount of ammonium, methylammonium, dimethylammonium, trimethylammonium, and tetramethylammonium salts. Signals arising from ubiquitous alkali-metal ions with varying abundances are due to sodium- and potassium-ion complex formation.

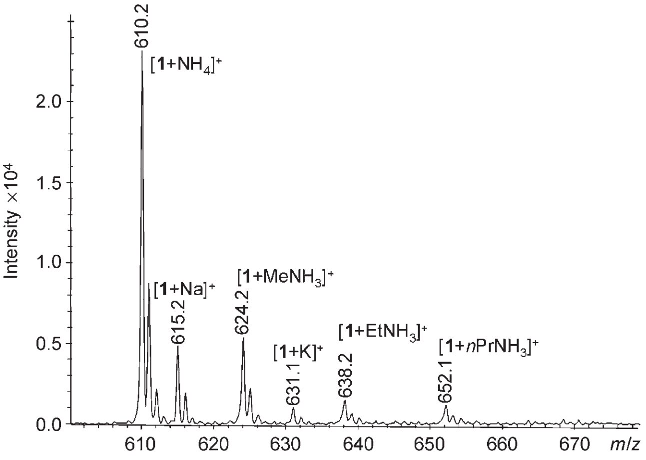

Figure 3. Electrospray mass spectrum of the tetramethylcavitand (X) in a mixture with an equimolar amount of ammonium, methylammonium, ethylammonium, and *n*-propylammonium salts. Signals arising from ubiquitous alkali-metal ions with varying abundances are due to sodium- and potassium-ion complex formation.

Experimental Section

The tetramethylcavitand **1** was prepared as described in the literature.[34] ESI mass spectra were recorded by using an Esquire 3000 ion-trap mass spectrometer (Bruker Daltonik GmbH, Bremen, Germany) equipped with an offline nano ESI source. Samples were introduced by using nanospray needles. Nitrogen served as both the nebulizer gas and the dry gas. Nitrogen was generated by a Bruker nitrogen generator NGM 11. Helium served as cooling gas for the ion trap. The spectra shown here were recorded by using the Bruker Daltonik esquireNT 5.1 esquireControl software by the accumulation and averaging of several single spectra. Data Analysis software 3.1 was used for processing the spectra. The tetramethylcavitand **1** was dissolved in chloroform (about $50\,pmol\,\mu L^{-1}$). This solution was mixed (1:1) with an equimolar mixture of different ammonium chlorides (each, $100\,pmol\,\mu L^{-1}$) in methanol.

Conclusion

A series of host–guest complexes for the cavitand with different ammonium cations was investigated theoretically at the DFT (RI-BP86 and B3LYP) level of approximation. The optimized structures reflect different modes of complexation. Only in the cases of the ammonium cations RNH_3^+ (R = H, Alkyl), does the nitrogen dive deeply into the cavitand cavity ("ammonium inside" complexation mode). The introduction is characterized by highly negative reaction energies that decrease as the number of methyl groups at nitrogen increases. For ammonium cations

NMe_nH_{4-n} ($n=2$–4), an “alkyl inside” complexation mode is found. In these cases, the exothermic complexation energies are small. The theoretical data are in line with the electrospray mass spectrometry results. The tetramethylammonium cation or other quaternary ammonium cations with larger alkyl substituents do not form stable aggregates with the cavitand. We have also demonstrated the potential of the DFT methods in predicting the stability of interesting host–guest complexes and descriptions of their structure.

Acknowledgements

This work was supported by the Deutsche Forschungsgemeinschaft (SFB 613). Computation time was generously donated by the Rechenzentrum of the Max-Planck Institut at Munich.

---

[1] a) C. D. Gutsche, *Calixarenes*, RSC, Cambridge, **1989**; b) C. D. Gutsche in *Inclusion Compounds, Vol. 4* (Eds.: J. L. Atwood, J. E. D. Davies, D. D. MacNicol), Oxford University Press, Oxford, **1991**, pp. 27–63; c) C. D. Gutsche in *Large Ring Molecules* (Ed.: J. A. Semlyen), Wiley, New York, **1996**, pp. 309–343.

[2] a) *Calixarenes: A Versatile Class of Macrocyclic Compounds* (Eds.: J. Vicens, V. Böhmer), Kluwer, Dordrecht, **1991**; b) S. Shinkai, *Tetrahedron* **1993**, *49*, 8933–8968; c) V. Böhmer, *Angew. Chem.* **1995**, *107*, 785–818; *Angew. Chem. Int. Ed. Engl.* **1995**, *34*, 713–745; d) A. Pochini, R. Ungaro in *Comprehensive Supramolecular Chemistry, Vol. 2* (Ed.: F. Vögtle), Pergamon, Oxford, **1996**, pp. 103–142; e) A. Ikeda, S. Shinkai, *Chem. Rev.* **1997**, *97*, 1713–1734.

[3] a) M. T. Blanda, D. B. Farmer, J. S. Brodbelt, B. J. Goolsby, *J. Am. Chem. Soc.* **2000**, *122*, 1486–1491; b) B. J. Goolsby, J. S. Brodbelt, E. Adou, M. Blanda, *Int. J. Mass Spectrom.* **1999**, *193*, 197–204; c) F. Allain, H. Virelizier, C. Moulin, C. K. Jankowski, J. F. Dozol, J. C. Tabet, *Spectroscopy*, **2000**, *14*, 127–139; d) J. M. J. Nuutinen, A. Irico, M. Vincenti, E. Dalcanale, J. M. H. Pakarinen, P. Vainiotalo, *J. Am. Chem. Soc.* **2000**, *122*, 10090–10100; e) M. C. Letzel, C. Agena, J. Mattay, *J. Mass Spectrom.* **2002**, *37*, 63–68.

[4] M. Mäkinen, P. Vainiotalo, K. Rissanen, *J. Am. Soc. Mass Spectrom.* **2002**, *13*, 851–861; M. Mäkinen, J.-P. Jalkanen, P. Vainiotalo, *Tetrahedron* **2002**, *58*, 8591–8596.

[5] For a review, see: J. C. Ma, D. A. Dougherty, *Chem. Rev.* **1997**, *97*, 1303–1324.

[6] a) J.-L. Sussman, M. Harel, F. Frolow, C. Oefner, A. Goldman, L. Toker, I. Silman, *Science*, **1991**, *253*, 872–879; b) A. Casnati, D. Sciotto, G. Arena in *Calixarenes 2001* (Eds.: Z. Asfari, V. Böhmer, V. Harrowfield, J. Vicens), Kluwer Academic, Dordrecht, **2001**, Chapter 24, and references therein.

[7] H.-J. Schneider, D. Güttes, U. Schneider, *J. Am. Chem. Soc.* **1988**, *110*, 6449–6454.

[8] J. M. Harrowfield, M. I. Ogden, W. R. Richmond, B. W. Skelton, A. H. White, *J. Chem. Soc. Perkin Trans. 2* **1993**, 2183–2190.

[9] J. L. Atwood, L. J. Barbour, P. C. Junk, W. Orr, *Supramol. Chem.* **1995**, *5*, 105–108.

[10] G. Arena, A. Casnati, A. Contino, F. G. Gulino, D. Sciotto, R. Ungaro, *J. Chem. Soc. Perkin Trans. 2* **2000**, 419–423.

[11] A. Irico, M. Vincenti, E. Dalcanele, *Chem. Eur. J.* **2001**, *7*, 2034–2042.

[12] A. Ghoufi, C. Bonal, J. P. Morel, N. Morel-Desrosiers, P. Malfreyt, *J. Phys. Chem. B* **2004**, *108*, 5095–5104.

[13] F. Perret, J.-P. Morel, N. Morel-Desrosiers, *Supramol. Chem.* **2003**, *15*, 199–206.

[14] a) G. Arena, A. Casnati, A. Contino, G. G. Lombardo, D. Sciotto, R. Ungaro, *Chem. Eur. J.* **1999**, *5*, 738–744; b) A. Mendes, C. Bonal, N. Morel-Desrosiers, J. P. Morel, P. Malfreyt, *J. Phys. Chem. B* **2002**, *106*, 4516–4524.

[15] W. Koch, M. C. Holthausen, *A Chemist's Guide to Density Functional Theory*, Wiley-VCH, **2001**.

[16] A. B. Rozhenko, W. W. Schoeller, M. Letzel, B. Decker, C. Agena, J. Mattay, *J. Mol. Struct. (THEOCHEM)* **2005**, *732*, 7–20.

[17] M. C. Letzel, B. Decker, A. B. Rozhenko, W. W. Schoeller, J. Mattay, *J. Am. Chem. Soc.* **2004**, *126*, 9669–9674.

[18] A. D. Becke, *Phys. Rev. A* **1988**, *38*, 3098–3100.

[19] J. P. Perdew, *Phys. Rev. B* **1986**, *33*, 8822–8824.

[20] a) B. I. Dunlap, J. W. Conolly, J. R. Sabin, *J. Chem. Phys.* **1979**, *71*, 4993–4999; b) O. Vahtras, J. Almlöf, M. W. Feyereisen, *Chem. Phys. Lett.* **1993**, *213*, 514–518; K. Eichkorn, O. Treutler, H. Öhm, M. Häser, R. Ahlrichs, *Chem. Phys. Lett.* **1995**, *240*, 283–289.

[21] R. Ahlrichs, M. Bär, M. Häser, H. Horn, C. Kölmel, *Chem. Phys. Lett.* **1989**, *162*, 165–169; R. Ahlrichs, M. von Arnim in *Methods and Techniques in Computational Chemistry*, MET ECC-95 (Eds.: E. Clementi, G. Corongiu), STEF, Cagliari, **1995**, p. 509 ff.; see also www.turbomole.com, and references therein.

[22] A. Schäfer, H. Horn, R. Ahlrichs, *J. Chem. Phys.* **1992**, *97*, 2571–2577.

[23] P. Deglmann, F. Furche, R. Ahlrichs, *Chem. Phys. Lett.* **2002**, *362*, 511–518; P. Deglmann, F. Furche, *J. Chem. Phys.* **2002**, *117*, 9535–9538.

[24] Gaussian 03, Revision A.1, M. J. Frisch, G. W. Trucks, H. B. Schlegel, G. E. Scuseria, M. A. Robb, J. R. Cheeseman, J. A. Montgomery, Jr., T. Vreven, K. N. Kudin, J. C. Burant, J. M. Millam, S. S. Iyengar, J. Tomasi, V. Barone, B. Mennucci, M. Cossi, G. Scalmani, N. Rega, G. A. Petersson, H. Nakatsuji, M. Hada, M. Ehara, K. Toyota, R. Fukuda, J. Hasegawa, M. Ishida, T. Nakajima, Y. Honda, O. Kitao, H. Nakai, M. Klene, X. Li, J. E. Knox, H. P. Hratchian, J. B. Cross, C. Adamo, J. Jaramillo, R. Gomperts, R. E. Stratmann, O. Yazyev, A. J. Austin, R. Cammi, C. Pomelli, J. W. Ochterski, P. Y. Ayala, K. Morokuma, G. A. Voth, P. Salvador, J. J. Dannenberg, V. G. Zakrzewski, S. Dapprich, A. D. Daniels, M. C. Strain, O. Farkas, D. K. Malick, A. D. Rabuck, K. Raghavachari, J. B. Foresman, J. V. Ortiz, Q. Cui, A. G. Baboul, S. Clifford, J. Cioslowski, B. B. Stefanov, G. Liu, A. Liashenko, P. Piskorz, I. Komaromi, R. L. Martin, D. J. Fox, T. Keith, M. A. Al-Laham, C. Y. Peng, A. Nanayakkara, M. Challacombe, P. M. W. Gill, B. Johnson, W. Chen, M. W. Wong, C. Gonzalez, J. A. Pople, *Gaussian*, *Inc.*, Pittsburgh PA, **2003**.

[25] a) R. Ditchfield, W. J. Hehre, J. A. Pople, *J. Chem. Phys.* **1971**, *54*, 724–728; b) W. J. Hehre, R. Ditchfield, J. A. Pople, *J. Chem. Phys.* **1972**, *56*, 2257–2261; c) P. C. Hariharan, J. A. Pople, *Mol. Phys.* **1974**, *27*, 209–214; d) P. C. Hariharan, J. A. Pople, *Theor. Chim. Acta* **1973**, *28*, 213–222.

[26] A. D. Becke, *J. Chem. Phys.* **1993**, *98*, 5648–5652.

[27] C. Lee, W. Yang, R. G. Parr, *Phys. Rev. B* **1988**, *37*, 785–789.

[28] S. L. Mayo, B. D. Olafson, W. A. Goddard III, *J. Phys. Chem.* **1990**, *94*, 8897–8909.

[29] A. K. Rappé, C. J. Casewit, K. S. Colwell, W. A. Goddard III, W. M. Skiff, *J. Am. Chem. Soc.* **1992**, *114*, 10024–10035.

[30] J. J. P. Stewart, *J. Comput. Chem.* **1989**, *10*, 209–220; J. J. P. Stewart, *J. Comput. Chem.* **1989**, *10*, 221–264.

[31] A. Schäfer, C. Huber, R. Ahlrichs, *J. Chem. Phys.* **1994**, *100*, 5829–5835.

[32] VMD for WIN-32, Version 1.8.2 (Dezember, 4, 2003): W. Humpfrey, A. Dalke, K. Schulten, *J. Mol. Graphics* **1996**, *14*, 33–38.

[33] For this nomenclature, see F. A. Cotton, G. Wilkinson, *Advanced Inorganic Chemistry*, John-Wiley, New York, **1988**.

[34] J. R. Moran, S. Karbach, D. J. Cram, *J. Am. Chem. Soc.* **1982**, *104*, 5826–5828.

Received: December 5, 2005
Revised: June 6, 2006